A low-complexity microwave scanner for cerebrovascular diseases monitoring

URSI GASS 2023, Sapporo, Japan, 19 – 26 August 2023

A Low-complexity Microwave Scanner for Cerebrovascular diseases Monitoring

D. O. Rodriguez-Duarte*(1), C. Origlia(1), J. A. Tobon Vasquez(1), R. Scapaticci(2),
G. Turvani(1), M. R. Casu(1), L. Crocco(2), and F. Vipiana(1)
(1) Dept. Electronics and Telecommunications, Politecnico di Torino, Torino, Italy; *e-mail: david.rodriguez@polito.it
(2) IREA-CNR, Institute for Electromagnetic Sensing of the Environment, National Research Council of Italy, Naples, Italy

Abstract

This work gathers the pathway from the design to the experimental testing of a microwave imaging prototype to monitor brain stroke in real-time conditions, approaching thus the electromagnetic inverse problem of retrieving a dielectric temporal variation within the head. To this end, it presents a low-complexity device consisting of twenty-two custom-made radiating elements working with a linear imaging algorithm based on distorted Born approximation and a truncated singular value decomposition, able to localize, identify and track the stroke evolution. The system is prototyped using a compact two-ports vector analyzer and electromechanical switching matrix. It is assessed experimentally via a mimicked hemorrhagic condition, demonstrating the system's capabilities to follow up centimetric confined variations, retrieving 3-D maps of the studied cases in real-time.

1 Introduction

Cerebrovascular diseases are a fast-evolving life-threatening medical condition that menaces millions of lives yearly, causing death or post-event short and long-term disabilities, having a higher incidence in the aged population [1]. It occurs when the oxygen-rich blood supply to the brain is interrupted or diminished by an artery blockage or a vessel's burst, inducing an ischemic (IS) or hemorrhagic stroke (HEM), and requiring a prompt medical response to mitigate the brain damage and its catastrophic repercussions.

The medical staff relies on visible symptoms and gold-standard imaging-based examinations such as magnetic resonance imaging (MRI) and computed tomography (CT), which are highly reliable, to diagnose and define the appropriate therapies. However, the current technologies lead to crucial unmet medical needs in terms of continuous follow-up and on-point diagnosis due to the lack of portability, long examination times, high cost, and use of ionizing radiation in the case of CT. These limitations open the door to complementary alternatives such as microwave imaging (MWI), which exploit the non-invasive and harmless nature of microwaves together with the current high-performance microwave hardware and computing power to overcome the constraints of traditional techniques, albeit its lower resolution, while allowing it to integrate into the pre-hospital and in-hospital emergency protocols smoothly, a strict medical requirement.

MWI principle relies on the contrast of the dielectric properties, i.e., permittivity and conductivity, exhibited by the healthy brain tissues and the stroke-affected when illuminated by low-power microwaves, to generate images of the body's internal structures using the resultant back-scattered signals. For instance, the properties of an IS-affected area decrease due to the reduction of the blood flow and, conversely, increase in the case of hemorrhage or bleeding.

MWI applied to brain stroke is reaching the named maturation stage of the typical evolutionary timeline of a medical imaging modality [2]. So, it is moving toward the clinical acceptance stage, characterized by the clinical focusing and technology refinement that results in application-based imaging systems, continued investigation, and early(pre) clinical trials as reflected by the recent appearance of devices in development or even prototypes in patient trials for stroke classification and imaging [3, 4]. In this context, and thanks to the extensive experience gained in more than a decade of research and strong collaboration covering from the conceptualization and feasibility study of brain stroke monitoring [5, 6], through the posing of rigorous system design methodology [7, 8], to the development of 2-D and 3-D multi-version devices [9–12], the authors illustrate the learnings via a prototyping recall and an experimental validation of compact low-complexity device for brain stroke imaging-based monitoring, being it the last version.

In the following, Section 2 describes the software and hardware components of the system, Section 3 presents an experimental monitoring validation, and, finally, Section 4 concludes and discusses the perspectives of the work.

2 Microwave Imaging System

A MWI system architecture is composed mainly of a device generating the impinged waves and then collecting the back-scatter response and an array of radiating elements transmitting and receiving the reflected and scattered signals processed by the imaging or classification algorithms.

Hence, this section describes the imaging-based monitoring algorithm in the first part and, then, the system's different hardware elements.

2.1 Real-time Monitoring Algorithm

As the proposed MWI device aims to monitor the evolution of the stroke-affected, we opt for a differential linear imaging algorithm that retrieves the dielectric contrast in almost real-time. It linearizes the scattering phenomena by adopting the distorted Born approximation [13] and is formulated as

$$\Delta S(t_0,t_1) = \frac{j\,\omega\,\varepsilon_b}{2\,a_p\,a_q} \int_{DoI} \mathbf{E}_p^{\text{ref}}(\mathbf{r}) \cdot \mathbf{E}_q^{\text{ref}}(\mathbf{r})\,\Delta\chi\,d\mathbf{r} \qquad (1)$$

where the measured variable, $\Delta S(t_0,t_1)$, is the differential scattering matrix between instants t_0 and t_1, with the differential dielectric contrast, the unknown variable, $\Delta\chi(t_0,t_1) = (\varepsilon(t_1)-\varepsilon(t_0))/\varepsilon_b$, on a domain of interest, DoI; $\varepsilon(t_n)$ is the complex permittivity distribution, and b indicates a reference background scenario. Also, j is the imaginary unit, $\omega = 2\pi f$ is the angular frequency, and a_p and a_q are the incoming root-power waves given at the p-th and q-th antenna ports, respectively. The symbol "$\cdot$" denotes the dot product, and $\mathbf{E}_p^{\text{ref}}$, $\mathbf{E}_q^{\text{ref}}$ are the fields radiated by the p-th and q-th antenna.

Equation (1) considers, first, the space-concentrated nature of the stroke morphology and the controlled examination time frame, allowing it to assume a small and weak field perturbation. Second, it distorts the problem to a reference scenario that contains a well-modeled system but a simplified anthropomorphic head model, considering the limited morphological a-priori information about the patients. Specifically, we consider a reference scene with a homogeneous anthropomorphic head filled with average brain material and a highly realistic model of the MWI system, which is employed to compute the field distribution via an in-house finite element method (FEM) solver [14].

Then, to obtain the contrast, (1) must be inverted. However, due to the underlying ill-posedness of the linear inverse problem, it is ill-conditioned, and its direct inversion is impossible. Accordingly, (1) is inverted by adopting the truncated singular value decomposition (TSVD) approach [15] as

$$\Delta\chi(\mathbf{r}) = \mathcal{L}^{-1}\{\Delta S(t_0,t_1)\} = \sum_{n=1}^{L_t} \frac{1}{\sigma_n} \langle \Delta S, u_n \rangle\, v_n, \qquad (2)$$

where $\mathcal{L}$ is the compact representation of the discretized operator, σ_n, u_n and v_n are the n-th singular value, right and left singular vectors, respectively, and L_t is the truncation index acting as a regularizer, which is set henceforth to n-th when σ_n/σ_1 is higher than -30 dB. This guarantees a good trade-off between enough information and fewer noise disturbances.

Notice that the SVD computation and building of the imaging operator are done offline. Instead, the contrast retrieval is done in time, taking a couple of seconds on a standard laptop. Moreover, considering the unavoidable manufacturing tolerance of the antennas tends to destabilize the idealized operator where all the antennas are assumed identical, the imaging operator is built on the transmission coefficients.

Here, it is worth recalling that the amount of information would be limited using this technique. So, it is not expected that it can arrive directly at the actual constitutive values of complex permittivity, as an iterative method does. However, the retrieved maps contain enough information to be able to determine and indicate qualitatively:

- the *detection of a contrast variation*, indicating if there was a change in the stroke-affected area with respect to a first measured scenario;
- the *localization*, signaling the position within the head of the variation, which is vital from the medical point of view;
- the *shape retrieval*, presenting graphically the volume variation;
- the *contrast sign* that may indicate the clinical change of state of the stroke-affected area.

All four listed data might be essential from the medical perspective.

Moreover, in addition to the aforementioned imaging algorithm, we employ different calibration and artifact removal techniques that allow working with measured data. More details are described in [11, 12].

2.2 Microwave Scanner

The microwave scanner comprehends all the different hardware components of the system, as shown in Fig. 1. It includes the control unit (a standard laptop in this case), which performs the imaging and addresses the electromechanical switching matrix and the 2-ports compact-factor vector analyzer (VNA, Keysight P9375A). The switching matrix interfaces the VNA ports with each of the 22 antennas, allowing a multi-view configuration. Then, the system collects a full 22×22 scattering matrix, arranging sequentially 2×2 segments in post-processing, which is a suitable assumption considering the scanning times are much slower than the stroke evolution. To ensure an optimal trade-off between signal-to-noise ratio and measurement time, the VNA was set with an input power of 0 dBm and the intermediate filter (IF) to 100 Hz. This configuration permits the system to collect the complete scattering matrix in about 5 minutes, noticing that the measuring time is mainly dictated by the mechanical switching time.

The last piece of the system is the radiating element, the antenna module here. It is designed to work around 1 GHz

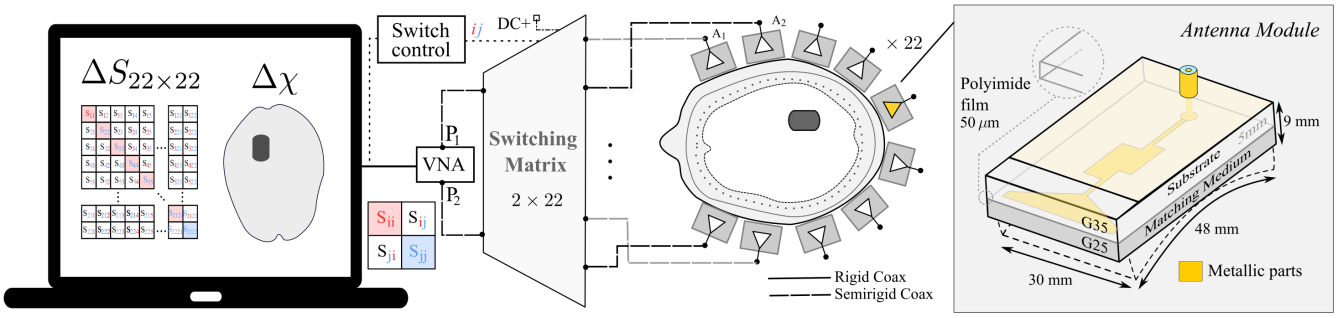

Figure 1. Scheme of the microwave scanner and the antenna module.

[12], using a flexible matching medium that improves the electromagnetic (EM) penetration within the head and the spatial resolution. It extends the features of the antenna presented in [16], which conveniently removes the need for liquid matching and replaces it with a solid one, compacting the antenna extent by merging a monopole and a matching layer, dubbed "G35"and "G25", respectively, in a two-layer stack structure as shown on the left side of Fig. 1. To make both the antenna substrate and the matching, mixtures of urethane rubber and graphite powder are employed, which allows tuning the permittivity of the material, giving one more degree of freedom to the design process. For instance, G35 implies a mixture using 65 % volume rubber and 35 % graphite, and presents a relative permittivity, $\varepsilon_r = 13$, and conductivity, $\sigma = 0.18$ [S/m], at 1 GHz, respectively. On the other hand, the radiating part and the trimmed ground plane (GND) are printed on slabs of $50\mu m$ polyimide film, the former being a triangular-shaped radiating element back-fed by a coaxial cable and a two-stubs line conceived to improve the antenna matching at the port. By last, twenty-two modules are placed conformally to the upper part of the head, adjusting each to the head curvature thanks to its flexibility and compact format, reaching full coverage of the brain area. Additional details on the antenna performance are found in [12].

3 Experimental Validation

To validate the prototype in a dynamic and more realistic situation, we reproduce a simplified, though meaningful, evolving intracranial hemorrhage in the lab. First, the head is mimicked using an anthropomorphic single-container phantom, 3-D printed in clear resin (polyester casting resin) and filled with a custom-made alcohol-water-based liquid with the properties of an average brain at 1 GHz, e.i., $\varepsilon_r = 45$ and $\sigma = 0.8$ [S/m], while the stroke is mimicked with a capsule-shaped balloon filled gradually by 20 cm^3 at a time, with mimicked blood, $\varepsilon_r = 63$ and $\sigma = 1.5$ [S/m]. All the materials properties were measured via the coaxial probe method aided by Keysight software suite [17].

The monitoring results present the normalized contrast amplitude as illustrated in Fig. 2, which clearly distinguishes the stroke evolution signaling the position, the trend, and the dimensions.

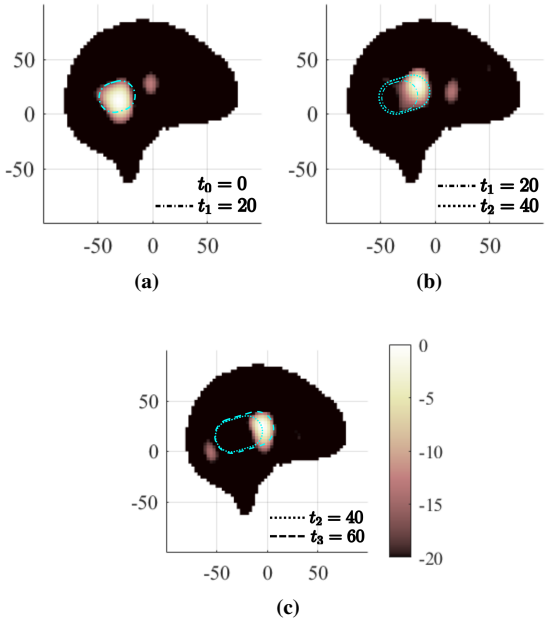

Figure 2. Monitoring of mimicked hemorrhage progression. Saggital view of the normalized reconstructed in dB of dielectric contrast sliced in the middle of the stroke region. (a): variation between a healthy to 20 cm^3 capsule-shaped stroke. (b): 20-40 cm^3. (c): 40-60 cm^3. The dimensions are in [mm], and the contour lines indicate an estimation of the respective stroke shapes.

4 Conclusion and Perspectives

The presented work converges software and hardware aspects of prototyping a low-complexity MWI scanner on the experimental validation of the device, resulting in real-time pathology monitoring. The results demonstrate the system's reliability in localizing the contrast variation and the centimetric sensitivity of about 1 cm, comparable with the theoretical resolution.

Looking into the future, we plan to extend the experimental validation using a more complex phantom, considering

multiple tissues. Moreover, the stroke classification and augmented resolution are being considered by integrating machine learning algorithms [18, 19].

Acknowledgments

This work was supported in part by the European Union's Horizon 2020 research and innovation program under the EMERALD project, Marie Skłodowska-Curie grant agreement No. 764479, in part by the project PON Research and Innovation "Microwave Imaging and Detection powered by Artificial Intelligence for Medical and Industrial Applications (DM 1062/21)," funded by the Italian Ministry of University and Research (MUR), and in part by the Agritech National Research Center, funded by the European Union Next-GenerationEU (Piano Nazionale di Ripresa e Resilienza (PNRR) – MISSIONE 4 COMPONENTE 2, INVESTIMENTO 1.4 – D.D. 1032 17/06/2022, CN00000022).

References

[1] C. W. Tsao, A. W. Aday, Z. I. Almarzooq, A. Alonso, A. Z. Beaton, M. S. Bittencourt, A. K. Boehme, A. E. Buxton, A. P. Carson, Y. Commodore-Mensah, *et al.*, "Heart disease and stroke statistics—2022 update: a report from the american heart association," *Circulation*, vol. 145, no. 8, pp. e153–e639, 2022.

[2] J.-C. Bolomey, *Crossed Viewpoints on Microwave-Based Imaging for Medical Diagnosis: From Genesis to Earliest Clinical Outcomes*, pp. 369–414. Cham: Springer International Publishing, 2018.

[3] A. Fhager, S. Candefjord, M. Elam, and M. Persson, "Microwave diagnostics ahead: Saving time and the lives of trauma and stroke patients," *IEEE Microwave Magazine*, vol. 19, no. 3, pp. 78–90, 2018.

[4] L. Guo, A. S. M. Alqadami, and A. Abbosh, "Stroke diagnosis using microwave techniques: Review of systems and algorithms," *IEEE Journal of Electromagnetics, RF and Microwaves in Medicine and Biology*, pp. 1–14, 2022.

[5] R. Scapaticci, L. D. Donato, I. Catapano, and L. Crocco, "A feasibility study on microwave imaging for brain stroke monitoring," *Progress in Electromagnetics Research B*, vol. 40, pp. 305–324, 2012.

[6] R. Scapaticci, O. Bucci, I. Catapano, and L. Crocco, "Differential microwave imaging for brain stroke followup," *International Journal of Antennas and Propagation*, vol. 2014, no. Article ID 312528, pp. 1–11, 2014.

[7] O. M. Bucci, L. Crocco, R. Scapaticci, and G. Bellizzi, "On the design of phased arrays for medical applications," *Proceedings of the IEEE*, vol. 104, no. 3, pp. 633–648, 2016.

[8] R. Scapaticci, J. Tobon, G. Bellizzi, F. Vipiana, and L. Crocco, "Design and numerical characterization of a low-complexity microwave device for brain stroke monitoring," *IEEE Transactions on Antennas and Propagation*, vol. 66, no. 12, pp. 7328–7338, 2018.

[9] J. A. Tobon Vasquez, R. Scapaticci, G. Turvani, G. Bellizzi, N. Joachimowicz, B. Duchêne, E. Tedeschi, M. R. Casu, L. Crocco, and F. Vipiana, "Design and experimental assessment of a 2D microwave imaging system for brain stroke monitoring," *International Journal of Antennas and Propagation*, no. Article ID 8065036, pp. 1–12, 2019.

[10] J. A. Tobon Vasquez, R. Scapaticci, G. Turvani, G. Bellizzi, D. O. Rodriguez-Duarte, N. Joachimowicz, B. Duchêne, E. Tedeschi, M. R. Casu, L. Crocco, and F. Vipiana, "A prototype microwave system for 3d brain stroke imaging," *Sensors*, vol. 20, no. 9, 2020.

[11] D. O. Rodriguez-Duarte, J. A. Tobon Vasquez, R. Scapaticci, G. Turvani, M. Cavagnaro, M. R. Casu, L. Crocco, and F. Vipiana, "Experimental validation of a microwave system for brain stroke 3-d imaging," *Diagnostics*, vol. 11, no. 7, 2021.

[12] D. O. Rodriguez-Duarte, C. Origlia, J. A. T. Vasquez, R. Scapaticci, L. Crocco, and F. Vipiana, "Experimental assessment of real-time brain stroke monitoring via a microwave imaging scanner," *IEEE Open Journal of Antennas and Propagation*, vol. 3, pp. 824–835, 2022.

[13] N. K. Nikolova, *Introduction to Microwave Imaging*. EuMA High Frequency Technologies Series, Cambridge University Press, 2017.

[14] D. O. Rodriguez-Duarte, J. A. T. Vasquez, R. Scapaticci, L. Crocco, and F. Vipiana, "Assessing a microwave imaging system for brain stroke monitoring via high fidelity numerical modelling," *IEEE Journal of Electromagnetics, RF and Microwaves in Medicine and Biology*, vol. 5, no. 3, pp. 238–245, 2021.

[15] M. Bertero and P. Boccacci, *Introduction to Inverse Problems in Imaging*. Inst. Phys., Bristol, U.K., 1998.

[16] D. O. Rodriguez-Duarte, J. A. T. Vasquez, R. Scapaticci, L. Crocco, and F. Vipiana, "Brick-shaped antenna module for microwave brain imaging systems," *IEEE Antennas and Wireless Propagation Letters*, vol. 19, no. 12, pp. 2057–2061, 2020.

[17] "N1500a materials measurement suite," 2022. Online.

[18] V. Mariano, J. A. Tobon Vasquez, M. R. Casu, and F. Vipiana, "Brain stroke classification via machine learning algorithms trained with a linearized scattering operator," *Diagnostics*, vol. 13, no. 1, 2023.

[19] A. Yago Ruiz, M. Cavagnaro, and L. Crocco, "An effective framework for deep-learning-enhanced quantitative microwave imaging and its potential for medical applications," *Sensors*, vol. 23, no. 2, 2023.